Journal of Materials Chemistry B

ROYAL SOCIETY OF CHEMISTRY

REVIEW

View Article Online
View Journal | View Issue

Cite this: J. Mater. Chem. B, 2020, 8, 2381

Effect of elasticity on the phagocytosis of micro/nanoparticles

Chenyang Yao,[a] Ozioma Udochukwu Akakuru,[a] Stefan G. Stanciu,[b] Norbert Hampp,[c] Yinhua Jin,[d] Jianjun Zheng,[d] Guoping Chen,[d] Fang Yang*[ac] and Aiguo Wu*[a]

Received 21st December 2019,
Accepted 3rd February 2020

DOI: 10.1039/c9tb02902h

rsc.li/materials-b

A broad range of investigation methods and frameworks are currently used to throughly study the elasticity of various types of micro/nanoparticles (MNPs) with different properties and to explore the effect of such properties on their interactions with biological species. Specifically, the elasticity of MNPs serves as a key influencing factor with respect to important aspects of phagocytosis, such as the clathrin-mediated phagocytosis, caveolae-mediated phagocytosis, macropinocytosis, and cell membrane fusion. Achieving a clear understanding of the relationships that exist between the elasticity of MNPs and their phagocytic processes is essential to improve their performance in drug delivery, which is related to aspects such as circulation lifetime in blood, accumulation time in tissues, and resistance to metabolism. Resolving such aspects is very challenging, and related efforts require using the right tools/methods, which are not always easy to identify. This review aims to facilitate this by summarizing and comparing different cell phagocytosis pathways, while considering various MNPs exhibiting different elastic properties, shape change capabilities, and their effect on cellular uptake. We conduct an overview of the advantages exhibited by different MNPs with respect to both *in vitro* and *in vivo* delivery, taking computational simulation analysis and experimental results into account. This study will provide a guide for how to investigate various types of MNPs in terms of their elastic properties, together with their biomedical effects that rely on phagocytosis.

1. Introduction

The outstanding advances that had occurred in the fields of micro- and nanotechnologies over the past couple of decades have led to rapid and consistent developments in functionalizing micro/nanoparticles (MNPs) for drug delivery. The effects of MNPs' properties such as size, shape, surface charge, and ligands on cell phagocytosis have been extensively studied.[1–3] Besides such fundamental characteristics, in recent years, the elastic properties of MNPs started to gain massive attention, since these have been found to play crucial roles in regulating various biological interactions, behaviors, and effects.[4–8] This is largely inspired by the fact that many cells and even viruses can achieve various biological functions by regulating their own mechanical properties. For example, it was discovered that macrophages can perceive small changes in red blood cell elasticity for selective phagocytosis.[9] In the context of drug delivery applications, the performance and success of MNPs are determined by the extent to which they can enter various biological species, *e.g.* cells, organelles, *etc.*[5] Therefore, comprehending the interaction of MNPs with cell membranes and achieving a clear understanding of their cellular uptake are critical to designing and producing safe and efficient next-generation materials for nanomedicine.

Although there is currently a consensus on the fact that the cellular uptake of MNPs is influenced by their elastic properties, the exact mechanism of the cellular phagocytosis is still not well resolved and some aspects are still under debate. For instance, some researchers proposed that harder MNPs are more likely to enter into cells,[10–12] while others argue the contrary.[13,14] Meanwhile, other experiments suggest that moderate elasticity is in fact the optimal condition for MNPs to be subjected to cellular uptake.[15–17] Considering the existence of such contradictory views on the subject, in this article, we summarize recent works addressing this topic, which we believe to be important for offering a perspective over the issues that still need to be clarified in order to design safer and better MNP functionalization strategies.

To be more specific, until now, researchers referred mainly to two aspects in order to analyze and explain the effects of

[a] *Cixi Institute of Biomedical Engineering, CAS Key Laboratory of Magnetic Materials and Devices & Key Laboratory of Additive Manufacturing Materials of Zhejiang Province, Ningbo Institute of Materials Technology and Engineering, Chinese Academy of Sciences, Ningbo 315201, P. R. China. E-mail: yangf@nimte.ac.cn, aiguo@nimte.ac.cn*
[b] *Center for Microscopy-Microanalysis and Information Processing, University Politehnica of Bucharest, Bucharest 060042, Romania*
[c] *Fachbereich Chemie, Philipps Universität Marburg, Marburg, 35032, Germany*
[d] *HwaMei Hospital, University of Chinese Academy of Sciences, 315010, P. R. China*

MNP elasticity on cellular uptake, namely their shape and the occurring phagocytic pathways owing to MNP shape. In this work, we reviewed important works addressing this subject and discuss the reasons for which these two aspects are believed to be of great importance in regulating cellular uptake as a function of MNP elasticity. Our attention is focused on both experimental work and theoretical studies that have been carried out based on simulations, which we believe to be important for achieving a good understanding of the considered subject. A detailed discussion on the available methods for the synthesis and control of MNPs, effect of MNP elasticity on their circulation in the blood, and solid tumor permeability has been extensively addressed in other works.[11,18–20]

2. Basic terms and methods for measuring elasticity

The mechanical properties of materials are often described by related properties such as elasticity, stiffness, hardness, ductility, toughness, *etc.* (Fig. 1). These different terms describe unique physical parameters,[21] which can be assessed by various/distinct characterization methods. Comparing the outputs of different studies addressing the mechanical properties of MNPs from different perspectives is therefore not easy. The internalization of MNPs is primarily controlled by elasticity and stiffness. In physics, elasticity is used to describe the ability of a material to resist stress-induced deformation and to return to its original state when stress is removed. For linear isotropic materials, elasticity includes Young's modulus and shear modulus, usually expressed as modulus of elasticity (N m^{-2} or Pa). Young's modulus is the ratio between the uniaxial tensile/compressive stress applied to the material and the corresponding strain along the stress direction. On the other hand, the shear modulus is the ratio of the shear stress to the corresponding shear strain of the material. Moreover, stiffness, another property of MNPs that is considered to play an important role in cellular uptake, characterizes the ability of the material to resist deformation at the initial load. The main difference between the two properties is that elasticity is an intrinsic property of the material, while stiffness is a broad property that takes the geometry (size and shape) of the material into account. In addition, the stiffness of a material encompasses compression, tensile, bending, and torsional stiffness. As the most common force applied to MNPs is compression, and therefore Young's modulus and compression stiffness represent the physical features that we focus on most intensively in this review.

The quantitative measurement of the physical properties of MNPs is a key factor in assessing and predicting their performance in biomedical applications. At present, the elasticity and stiffness of MNPs are mainly measured *via* atomic force microscopy (AFM). The accuracy of the measurement depends mainly on the geometry of the probe's apex, namely the tip,[22] scanning mode and the calculation model. Table 1 summarizes the most common ways of measuring mechanical properties of

Chenyang Yao

Chenyang Yao obtained his bachelor degree in Materials Chemistry from Central South University, Changsha, China in 2017 and is now studying at the Cixi Institute of Biomedical Engineering, Ningbo Institute of Materials Technology and Engineering, Chinese Academy of Sciences (CIBE-NIMTE).

Fang Yang

Fang Yang is currently acting as an Associate Professor at the Cixi Institute of Biomedical Engineering, Ningbo Institute of Materials Technology and Engineering, Chinese Academy of Sciences (CIBE-NIMTE) and is involved in multiple research projects related to nanobiomaterials and their biological effect. His Bachelor in Physics (2010), Masters of Physics (2012) and PhD in Chemistry (2016) titles were awarded by the Phillips University of Marburg (PUM) in Germany. Throughout his studies, Fang was also deeply involved in research: 2008–2012 Research Assistant at the Biophotonics Department of PUM; 2010–2012 Researcher at the Biophysical Chemistry Department of PUM; 2012–2016 full time Researcher and PhD student at the Biophysical Chemistry department of PUM.

Aiguo Wu

Aiguo Wu received his PhD from the Changchun Institute of Applied Chemistry, Chinese Academy of Sciences (CAS), China, in 2004. He started his independent career working for NIMTE after taking up his research associate appointment at Northwestern University, USA and his postdoctoral positions at Caltech, USA and the University of Marburg, Germany. His research is focused on the synthesis of nanomaterials and their biomedical applications in biosensors, bioimaging, and drug delivery. He has authored over 180 scientific publications and has received some scientific awards and honors. The published papers have been cited by others more than 7300 times with an H-index of 46.

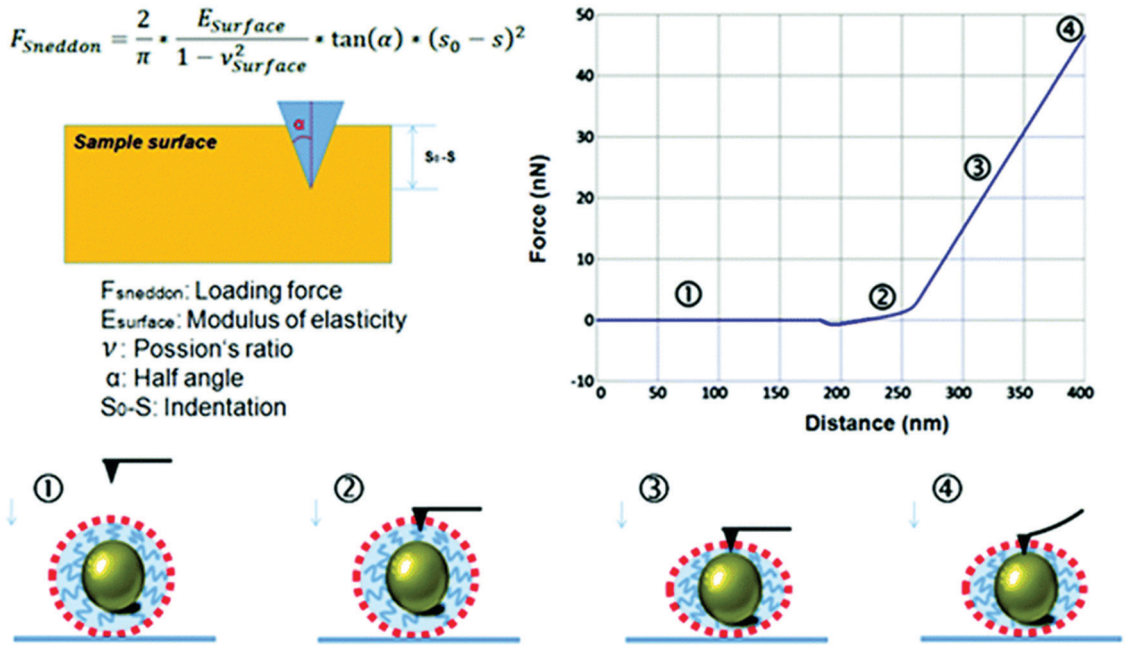

Fig. 1 Measuring the mechanical response of the NPs during the approach and the retraction of the AFM probe. Figure adapted from Sun *et al.* (2018). Copyright 2018 Royal Society of Chemistry.

Table 1 Different methods for measuring MNP elasticity *via* AFM

MNP	Probe shape	Scanning mode	Calculation model	Ref.
Hollow periodic mesoporous organosilica (~300 nm)	Standard (steep) Front angle: 25 ± 2.5° Back angle: 17.5 ± 2.5° Side angle: 20 ± 2.5°	PeakForce QNM mode	Hertzian model	81
Nanolipogels (~100 nm)	Four sided pyramid tips	Contact mode	Hertz equation	69
PLGA core–(lipid shell) NPs (~200 nm)	Not reported	PeakForce QNM mode	Young's modulus in PeakForce QNM mode	17
DNA-loaded polypeptide particles (~1 μm)	A conical indenter Full tip cone angle 40°	Contact mode	Hertz–Sneddon relationship	16
DEA–HEMA hydrogel spheres (~170 nm)	Conical indenter	Contact mode	Hertz model	15
Lipid–polymer hybrid NPs (~80 nm)	Rotated (symmetric) Front angle: 15 ± 2.5° Back angle: 25 ± 2.5° Side angle: 17.5 ± 2.5°	PeakForce QNM mode	Young's modulus in PeakForce QNM mode	12
P–L and P–W–L NPs (40 nm)	Not reported	PeakForce QNM mode	Derjaguin, Muller, Toropov (DMT) model	64
Discoidal polymeric nanoconstructs (~2 μm)	Quadratic pyramid indenter	Quantitative imaging (QI) mode	Hertz model	90

MNPs *via* AFM. Different AFM tip shapes have been used for this purpose, ranging from conical indenters to four sided pyramid tips. For all cases, the tip's radius of curvature determines the resolution of detection. Generally, the smaller the size of the MNPs, the smaller the radius of curvature required to accurately assess their mechanical properties. The tip's tilt angle also affects the detection of irregular objects. However, the most common shape of elastic MNPs developed to be functionalized for biomedical applications is the sphere, hence the influence of this latter parameter is not significant. With respect to the scanning modes most commonly used for assessing the elastic properties of MNPs, approximately half of the experiments addressing such purposes employed the contact mode, but PeakForce Quantitative Nanomechanical mapping is also widely used. This latter scanning mode can be regarded as being more advanced compared to the contact mode, since it can distinguish between various distinct nanomechanical properties, including elasticity, adhesion dissipation, and deformation. In addition, it is compatible with a wider range of samples compared to the contact mode, ranging from extremely soft materials (~1 kPa) to hard metals (100 GPa). This range practically covers most of the elastic MNPs synthesized in various laboratories for biomedical applications. With respect to the calculation modes that are most commonly used in experiments dealing with mechanical property assessment, most studies reported to date employed the Hertz model. This model considers a linear elastic sphere, regardless of the surface forces and adhesion. The calculation depends only on the loading force, Poisson's ratio, radius of the indenter,

and depth of the indentation.[21] However, in the case of small particles (<50 nm), the pressure exerted by the probe is also important to be considered. Therefore, the DMT model can serve as a better option for such MNPs. Furthermore, the Sneddon equation, which considers a rigid conical shape on an elastic half-space, is also very suitable under the corresponding conditions. In general, employing different detection/calculation methods can impact the obtained results numerically, but the overall trend of elasticity in experiments focused on comparing different versions of a specific or different MNPs will not change. However, comparing results obtained in distinct studies that employed different detection methods should be done with caution.

In this paper, different types of MNPs are categorized using three generic terms to describe their elastic properties, soft, intermediate, and hard, respectively. Since the materials addressed in each study are different, the reported elasticity and stiffness values will not be directly compared. However, the causes behind the performance of soft and hard MNPs in the process of cell phagocytosis are discussed in detail.

3. Phagocytic pathways mediated by elasticity

Although MNPs are small in size, they are polar molecules and hence cannot diffuse through the cell membrane but, instead, mainly enter the cells through the endocytic pathway.[23,24] Over the years, a wide variety of MNPs have been discovered that are endocytosed by cells. These coexist and function in different types of cells. In nanomedicine, the rate and extent of MNP phagocytosis by cells determine their performances at the treatment sites. Many recent experiments have shown that differences in the elasticity of MNPs may affect the way they are internalized into the cells. Therefore, understanding the underlying mechanisms involved in cell phagocytosis is crucial in assessing the fate of MNPs during internalization. In this section, we first introduce some possible ways of internalizing MNPs, and then discuss a series of relevant experimental approaches that have been implemented to date in the purpose of analyzing and understanding occurring mechanisms.

3.1. Classification of cell phagocytosis

In all cell types, small particles, with sizes in the nanometer range, are internalized by pinocytosis.[25] The pinocytosis effect is independent of the needs of cells and proceeds in a continuous manner in almost all cells. The role of pinocytosis can be subdivided into clathrin-mediated endocytosis, caveolae-mediated endocytosis, macropinocytosis, and others.[26,27]

Clathrin-mediated endocytosis was first discovered in electron micrographs for the study of yolk protein uptake in Aedes aegypti mosquitoes as a major component of the "hair follicle".[28,29] Clathrin-mediated endocytosis is an entry mechanism that internalizes specific molecules into cells. Its role is to help cells to take up plasma membrane components and nutrients, including low-density lipoprotein receptor cholesterol and iron with transferrin.[26,30–32] Clathrin acts as a heterodimer trimer, each unit consisting of a heavy chain and a light chain forming a triangle.[33] These triangles can be assembled into a lattice structure around the vesicles, and the adaptor proteins are used to link the endocytic cargo to the clathrin shell.[34] Briefly, clathrin-mediated endocytosis involves the identification of the cargo and the assembly of the coating, followed by the membrane invagination, and finally the pinch-deformed depression. After cleavage from the cell membrane, a series of accessory proteins are responsible for holding the actin cytoskeleton together and for coordinating the migration of the cargo into the body.[35] The cargo that is endocytosed into the cell eventually reaches the lysosome through the endolysosomal pathway.[36–38] In the case of NPs, these are internalized depending on the preferential ingestion by cells.

A previous study has shown that clathrin-mediated endocytosis and caveolae-mediated endocytosis may be helpful in the uptake of NPs with a negatively charged surface, while macropinocytosis appears to favour NPs with positive charges.[39] For example, un-modified gold NPs (positively charged) are mediated by macropinocytosis, clathrin-mediated endocytosis, and caveola-mediated endocytosis, while PEG-coated NPs (negatively charged) primarily enter into cells by clathrin-mediated endocytosis and caveola-mediated endocytosis.[40]

The caveola is a cholesterol-rich plasma membrane structure characterized by a unique morphology (60–80 nm cup-shaped invagination) and characteristic proteins.[41] The transport of caveolae is controlled by the cytoskeleton, and the caveola of the cell membrane has been shown to interact with actin filaments and stress fibers, microtubules, and intermediate filaments.[42–45] The caveolae exist in endothelial, epithelial and adipose cells, muscles, and fibroblasts[46–48] and those present in the cell membrane are usually 50–80 nm in size and consist of the membrane protein caveolin-1, giving them a bottle-like structure. Once the caveolae of the cell are detached from the plasma membrane, they fuse with caveosomes. Caveosomes are able to bypass lysosomes and protect the contents from degradation by hydrolases and lysosomes. Therefore, pathogens including viruses and bacteria are prevented from degrading by this route. This strategy is also applied in nanomedicine because the cargo that is mediated through the caveolae into the cell does not eventually enter the lysosome.[31,49]

Macropinocytosis describes a process in which a large number of fluid phases are engulfed by cells and in some cases, MNPs and bacteria are also collectively engulfed. It was originally described by Lewis as large phase-bright organelles originating from plasma membrane (PM) ruffles.[50,51] Macropinocytosis is actin-driven and caused by membrane wrinkles produced by growth factors or other signals, rather than cargoes. The formation of membrane processes is controlled by the small family Rho-GTPases and they fuse with the plasma membrane to form a large cell body that can internalize the surrounding extracellular fluid.[31,51] A series of imaging techniques for cultured cells and cells in the liver indicated that NP uptake is dependent on macropinocytosis.[52–54] The endocytic transport mechanism of macropinocytosis is complex. For example, lipid NPs stimulate macropinocytosis but this stimulation depends on its initial clathrin-mediated endocytosis.[55]

The fusion of cell membranes is the basic process of life, being responsible for the highly regulated transport between cells and intracellular molecules.[56] In order to achieve fusion, it is necessary to overcome the energy barrier during membrane merging and subsequent membrane instability. However, the process of membrane fusion requires less time and energy compared to endocytosis.[57,58] Currently, membrane-fused systems and liposome-encapsulated drugs and genes are widely used in both *in vitro* and *in vivo* delivery. In this case, the drug-loaded carrier fuses with the cell membrane to deliver the drug directly into the cytoplasm.[59] Experimental studies have shown that the fusion activation energy between cell membranes is much lower than most predictions. This low energy value explains how to prevent spontaneous fusion between cells but allows the intercellular substance to be delivered once the fusion-inducing protein is in place.[60]

In addition, there are other methods of phagocytosis, such as clathrin/caveolae-independent endocytosis,[31] CLIC/GEEC,[61] and ARF6-dependent pathways.[62] The phagocytic pathways described above demonstrate some level of uncertainty as to which is faster or more important, but it is important to highlight that the difference in how the phagocytosis is achieved has an impact on the extent of the outcome.

3.2. Effects of MNP elasticity on different phagocytic pathways

When investigating the causes behind phagocytosis differences, researchers found that MNPs possessing non-identical elastic properties phagocytize in different ways (see Table 2). In general, harder MNPs are more likely to be endocytosed by cells compared to softer ones, a situation that was observed in macrophages, cancer cells or endothelial cells.[12,63,64] However, there are also some different phenomena due to which the internalization of softer or intermediate elastic MNPs was found to take place with more ease.[14,65,66] In an experiment reported by Myerson *et al.*, it was shown that softer lysozyme–dextran nanogels can easily target the plasmalemma vesicle associated protein (PLVAP) in the lungs of mice, indicating the role of the elastic properties of the material in optimizing the drug delivery vehicle.[67] The identified reason was that softer NPs are responsive to shear forces in the flow buffer and are hence capable of deforming and elongating into a porous environment (Fig. 2a and b). Therefore, in this experiment, softer NPs were more likely to enter the cell through caveola-mediated endocytosis.

Softer MNPs also induce different phagocytic pathways due to changes in their shape. Liu *et al.* found that the softer particles were more internalized and abundant in Hep G2 cancer cells using a HEMA hydrogel sphere with a size of about 1 μm and a bulk modulus of 16.7–155.7 kPa.[68] On studying the mechanism of phagocytosis (Fig. 2c), they observed that harder particles rely on clathrin-mediated endocytosis and caveola-mediated endocytosis, while softer particles rely on macropinocytosis.[68] This may be due to the fact that the softer MNPs are prone to deformation when they are in contact with the cells, resulting in a larger radius of curvature of the particles from the cellular point of view, thereby activating the phagocytic mode of cells.

Another recent study addressing a mouse model of breast cancer *in situ* found that tumor and normal cells have greater uptake of softer nanolipogels (<1.6 MPa), when referring to a defined period of time.[69] In the same study, it was observed that immune cells exhibit no significant difference in the uptake of different elastic nanolipogels, compared to the tumour cells, which favored the accumulation of the softest nanolipogels. The researchers found that harder nanolipogels enter the cell mainly through clathrin-mediated endocytosis methods, while softer nanolipogels not only have a clathrin-mediated approach, but also fuse cell membranes in a fast process that requires less energy[60] to enter the cells (Fig. 2d and e). This also explains why the softest nanolipogels accumulate most at the tumor site.

Furthermore, soft hydrogel NPs (~18 kPa) were introduced into macrophages by means of macropinocytosis, and hard (~211 kPa) NPs were internalized through clathrin-mediated endocytosis mechanisms (Fig. 2f). NPs with an intermediate value of the Young's modulus (36 kPa) simultaneously exhibit these two internalization methods (Fig. 2g). Reported experimental results showed that the two internalization modes of such NPs account for a higher probability for them to enter into macrophage cells.[15] It is well understood that the two internalization modes tend to coexist, instead of a single mode. Therefore, NPs of different materials and different elastic moduli can cause different phagocytosis modes, which contain clathrin-mediated endocytosis, caveola-mediated endocytosis, micropinocytosis and cell membrane fusion. Different phagocytic pathways lead to different degrees of internalization.

Table 2 Phagocytic pathways affected by the elastic properties of MNPs

Particle type	Phagocytic pathways	Cellular uptake results
HEMA hydrogel spheres (900–1300 nm)	Hard (156 kPa): clathrin-mediated endocytosis and caveolae-mediated endocytosis Soft (15 kPa): micropinocytosis	Softer particles internalized faster and in higher amounts in Hep G2 cancer cells[68]
Lysozyme–dextran nanogels (150–300 nm)	Hard (8.47 MPa): not reported Soft (67.88 kPa): caveolae-mediated endocytosis	Softer NPs can pass through endothelial cells in blood vessels to target PLVAP in the lungs[67]
Nanolipogels (~100 nm)	Hard (19 MPa): clathrin-mediated endocytosis Soft (4.5 kPa): clathrin-mediated endocytosis and membrane fusion	Soft nanolipogels accumulated significantly more in tumors[69]
DEA–HEMA hydrogel spheres (~170 nm)	Hard (211 kPa): clathrin-mediated endocytosis Intermediate (36 kPa): clathrin-mediated endocytosis and macropinocytosis Soft (18 kPa): micropinocytosis	Intermediate elasticity NPs show highest cell uptake[15]

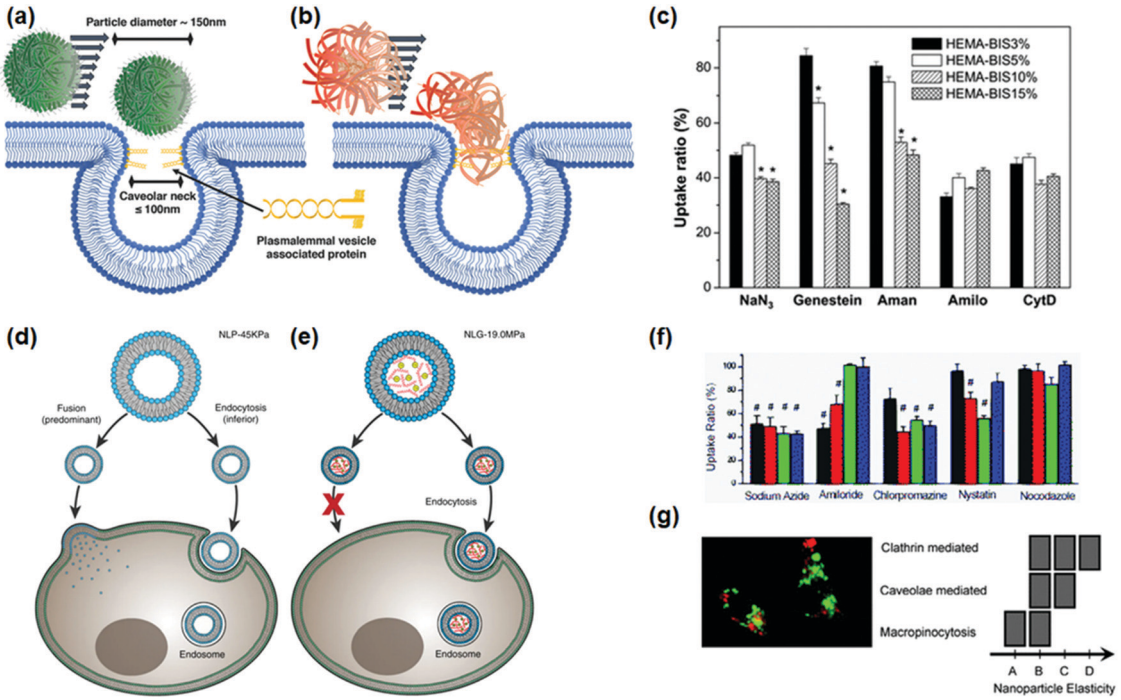

Fig. 2 Effects of MNP elasticity on different phagocytic pathways. (a) The geometry of caveolae limits PLVAP access for large rigid bodies. (b) Under mild shear force, nanogels reshape the flexible particle, and nanogels were shown to successfully target PLVAP at the caveolar entrance in mouse lungs. (c) Influence of pharmacological inhibitors on the uptake of different modulus hydrogel particles shows that harder particles rely on clathrin-mediated endocytosis and caveola-mediated endocytosis, while softer particles rely on macropinocytosis. (d) Soft NLP-45 KPa entering the cell has one more pathway: fusion as against Hard NLG-19 MPa (e). (f) The NPs of intermediate Young's modulus have two internalization modes and enter into macrophages the most. (a) and (b) adapted from Myerson *et al.* (2018). Copyright 2018 The Wiley-VCH. (c) adapted from Liu *et al.* (2012). Copyright 2012 Royal Society of Chemistry. (d) and (e) adapted from Guo *et al.* (2018). Copyright 2018 Springer Nature. (f) and (g) adapted from Banquy *et al.* (2009). Copyright 2009 Royal Society of Chemistry.

4. Effects of elasticity-induced shape changes on phagocytosis

The effect of MNP shape on cell phagocytosis has been widely discussed in earlier work.[70,71] Owing to the fact that most of the elastic MNPs synthesized for biomedical applications basically exhibit a spherical shape, the shape of soft NPs is prone to become ellipsoidal when they come in contact (or are coated) with the cell membrane. Therefore, in the case of such particles prone to shape modifications, the discussion on how their elasticity influences the phagocytosis also has an important component consisting of the particle shape influence on the outcome of this process.[72,73] A correct understanding of the shape modifications that elastic MNPs exhibit during phagocytosis is required to accurately comprehend the occurring uptake differences. This section first discusses the effects of different shapes of MNPs on cell phagocytosis, in particular of spheres and ellipsoids, and later focuses on the effects of different usually met shape deformations on the interaction between MNPs and cells during this process.

4.1. Effect of MNP shape on cell phagocytosis

Spheres and ellipsoids represent the two most commonly met shape models used to compare the effects of shape differences on cellular phagocytosis. Ellipsoid shapes are in general obtained by two fabrication methods: (i) by synthesis methods specifically designed to result in the ellipsoidal shape[74] and (ii) by mechanically squeezing spherical MNPs.[70] The effect of ellipsoidal shape on MNP internalization has been carefully studied in several important works, as discussed next.

In an earlier study, Paul *et al.* showed using real-time imaging techniques that polystyrene ellipsoids are phagocytosed by macrophages (RAW264.7) five times slower than spheres.[75] In a different study conducted by Doshi and Mitragotri, it was shown that rod-shaped or ellipsoidal spherical particles of 2–3 μm (the size range of common bacteria in nature) coated with mice IGg exhibit a greater adhesion to the surface of macrophages compared to spherical particles.[76] At the same time, Sharma *et al.* studied the behavior of endocytic spheroids, long ellipsoids, and spheroidal particles in macrophages, and found that the order of attachment to macrophages was oblong ellipsoid > oblate ellipsoid > sphere. However, the degree of internalization after attachment was found to have the following order: oblong > ellipsoid ≫ sphere > long ellipsoid, indicating that (i) NP attachment is an aspect of the phagocytic process; (ii) the order of NP attachment does not determine the order of phagocytosis; and (iii) the shape of the NPs alone affects cell attachment and internalization.[77] However, Zhang *et al.* found that spherical NPs were easier to be internalized by HeLa cells compared with ellipsoidal (including oblate ellipsoidal and prolate ellipsoidal) NPs, but more

difficult to bind with the cell surface.[78] Lu *et al.* also reported that nanorods show reduced cellular uptake compared to nanospheres, and in contrast, the larger contact area of nanorods resulted in greater membrane interaction.[79]

The uptake of ellipsoidal NPs has also been investigated in the context of spherical polymer NPs by means of a miniemulsion, to achieve ellipsoidal polymer NPs having the same volume but different aspect ratios.[80] By qualitatively and quantitatively studying the uptake behaviors of spheres and aspheric particles, it was found that the particles with ellipsoidal shape exhibit lower efficiency of cellular uptake compared to their spherical counterparts. An additional important finding of this study is that a negative correlation exists between the aspect ratio and the uptake rate, which was attributed to the larger average radius of the non-spherical particles adsorbed by cells.

4.2. Effect of the deformation of elastic MNPs on phagocytosis

When the elastic MNPs of spherical shape are in contact with cells, the softer MNPs are prone to becoming larger and ellipsoidal in shape. This transformation from spherical to ellipsoidal shape is a dynamic process, so the elasticity problem can better be described as a shape effect (Table 3). Different outcomes of the cellular uptake were considered to be dependent on shape, but it was found that a similar shape does not guarantee the same results, thus shape represents only a part of the contributing factors.[70] For example, in a study addressing the morphological transformation of PEG-modified solid or hollow silica NPs (233 MPa and 47 MPa) by MCF-7 cells, observed *via* transmission electron microscopy (Fig. 3a), it was found that soft NPs, whose shapes were modified from spherical to ellipsoidal, can enter MCF-7 cells more easily.[81] For soft NPs, the observed cellular uptake was found to be 26 times higher compared to harder NPs. However, other studies suggest the contrary, which translates that a general rule cannot be established, and that the problem is material specific. For instance, Yu *et al.* found that medium-elastic PLGA core (lipid shell) NPs (~50 MPa) demonstrated better mucosal and tumor-penetrating abilities compared to their soft and hard counterparts compared to some synthetic mucus penetration particles (MPPs).[17] The internalization process, which was investigated by molecular dynamics simulation and super-resolution microscopy, revealed that the hard (~110 MPa) NPs could not be deformed, while the excessively soft (~5 MPa) NPs deformed extensively, which hindered cellular interaction (Fig. 3b). Such discrepancies in the results of works addressing the problem of NP deformation impact on cellular uptake suggest that the occurring effect is not absolute. When soft NPs can be deformed into ellipsoids, the deformation is favorable, but when the shape change is large, the wrapping of the cell membrane may be hindered. Previously, similar results were found in an animal model, in an experiment that demonstrated that longer, softer, and more flexible filomicelles are significantly less internalized by macrophages compared to harder ones.[82]

Recently, Yu *et al.* found through super-resolution microscopy and molecular dynamics simulations that liposomes become elliptical near the phase transition temperature during diffusion in biohydrogels, a temperature- and stiffness-mediated rapid transport mechanism.[83] They showed that liposomes undergo dramatic changes in stiffness near the phase transition temperature, and that liposomes with phase transition temperatures near body temperature show enhanced cellular uptake in mucus (Fig. 3c). In addition, small unilamellar vesicles with intermediate rigidity were found to show better extratumoral matrix diffusion and multicellular spheroid penetration and retention compared to their harder or softer counterparts, which contributes to improving tumor suppression.[84] Liposomes with intermediate rigidity were able to change to rod-like shapes in multicellular spheroids (MCSs), enabling fast transport in tumor tissues (Fig. 3d). In contrast, stiff liposomes hardly deformed, whereas the shapes of soft liposomes changed irregularly, which slowed their MCS penetration. Hence, a general rule cannot be established, and the problem is material specific, but we can be sure that the shape changes of MNPs definitely have an (intricate) influence on the cellular uptake.

5. Computational simulation analysis

Although experimental methods are very important for achieving a clear understanding of the effects of elasticity on the internalization

Table 3 Effect of elasticity-induced shape changes on phagocytosis

Particle type	Shape changes	Cellular uptake results
Hollow periodic mesoporous organosilica (~300 nm)	Spherical-to-oval morphology change	The deformable hollow periodic mesoporous organosilica can easily enter into MCF-7 cells, resulting in a 26-fold enhancement in cellular uptake[81]
PLGA core–(lipid shell) NPs (~200 nm)	Semi-elastic NPs deform into ellipsoids. In contrast, rigid NPs cannot deform, and overly soft NPs are impeded	Orally administered semi-elastic NPs efficiently overcome multiple intestinal barriers, and lead to increased bioavailability of doxorubicin (DOX) (up to 8 folds) compared to the DOX solution[17]
Filomicelles (0.5–5 μm)	Filomicelles were ten times longer than their spherical counterparts	Under fluid flow conditions, spheres and short filomicelles are more easily absorbed by cells than longer filaments[82]
Small unilamellar vesicles (~100 nm)	The intermediate liposomes were able to transform to a rod-like shape. In contrast, hard liposomes hardly deformed, whereas soft liposomes changed their shape irregularly	The intermediate liposomes stimulated fast transport, on the contrary, hard and soft liposomes slowed their penetration in tumor tissues[84]
Liposomes (~400 nm)	Liposomes frequently deform into an ellipsoidal shape near the phase transition temperature	Compared to those with higher or lower transition temperatures, liposomes with transition temperature around body temperature show enhanced cellular uptake in mucus-secreting epithelium due to deformation[83]

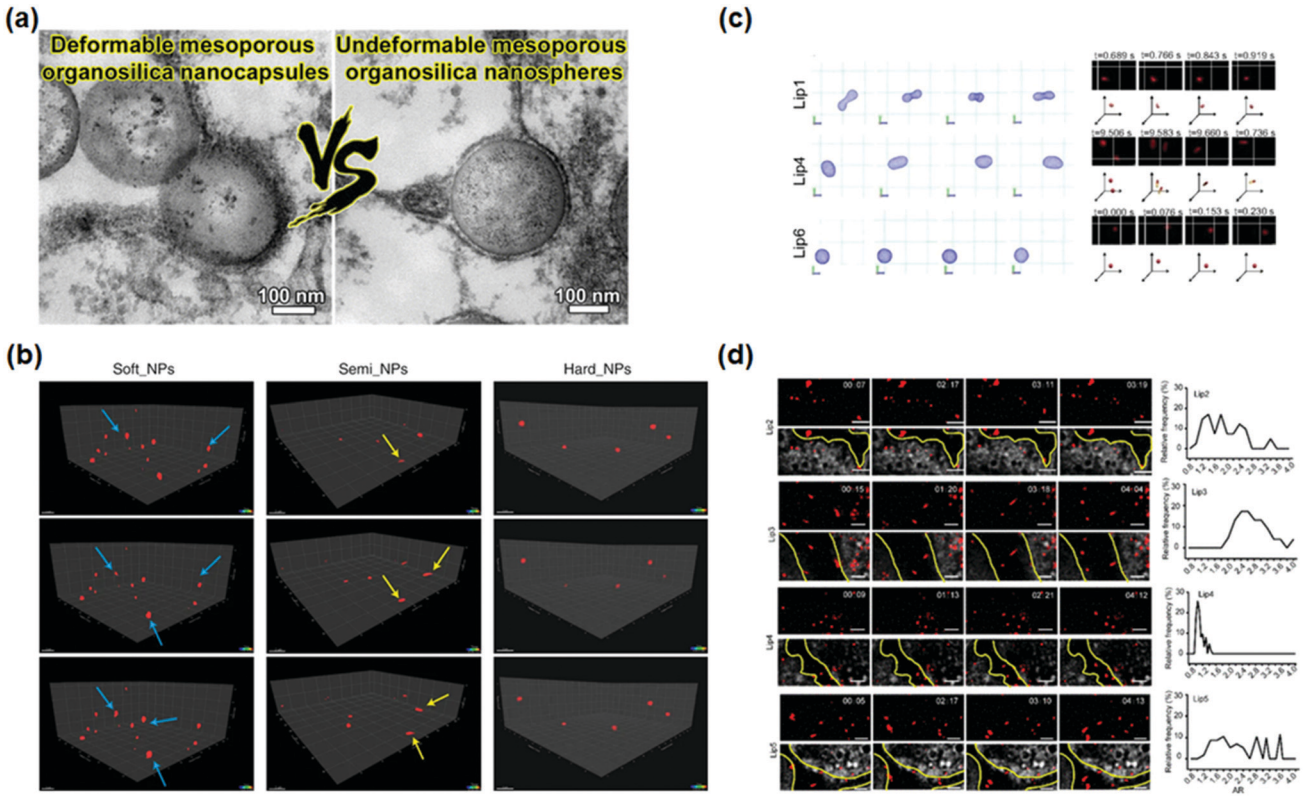

Fig. 3 Effect of the deformation of elastic NPs on phagocytosis. (a) TEM images of the uptake processes of organosilica nanocapsules by MCF-7 cells at 37 °C. Deformable mesoporous organosilica nanocapsules have a spherical-to-oval morphology change. (b) Snapshots and trajectories of NPs in rat intestinal mucus, as imaged *via* Airyscan microscopy. Soft NPs deformed into irregular shapes (blue arrows). Semi-elastic NPs deformed into ellipsoids (yellow arrows). Scale bars: 2 μm. (c) STED microscopy images showing the position and deformation of the liposomes in mucus. The corresponding 3D schematic drawings in the panel (*xyz*-axis) are drawn below the STED images. (d) STED microscopy images showing *in vitro* liposome deformation and movement in BxPC-3-HPSC MCS. Scale bars: 1 μm. (a) adapted from Teng *et al.* (2018). Copyright 2018 American Chemical Society. (b) adapted from Yu *et al.* (2018). Copyright 2018 Springer Nature. (c) adapted from Yu *et al.* (2019). Copyright 2019 National Academy of Sciences. (d) adapted from Dai *et al.* (2019). Copyright 2019 American Chemical Society.

of NPs into cells and for assessing the actual results occurring in reality, computational simulations are also very important. They can explain from another perspective why elasticity can affect the transport process of NPs. An illustrative example is the landmark work of Yi *et al.*, where both theoretical analysis and molecular simulation were performed with respect to elastic cylindrical (2D) or spherical particles (3D).[85] The authors selected several important parameters such as vesicle size, adhesion energy, surface tension of the membrane, and the bending stiffness ratio between the vesicle and the membrane to study the degree of particle wrapping by the cell membrane. They found that harder particles are easier to be completely enclosed compared to softer particles. Furthermore, they argue that because softer particles experience less energy changes during wrapping, they may be more advantageous as complete wrapping is not necessary (Fig. 4a). Other works dealing with simulations reveal additional important aspects. For instance, the difficulty in the internalization of softer NPs can be attributed to their ability to generate an additional energy barrier due to deformation. In the work of Sun *et al.* (Fig. 4b and c), molecular dynamics simulations were used to reproduce the internalization of NPs into cells.[64] In compliance with the Canham–Helfrich framework,[86] the authors first set a dimensionless parameter σ, and then mainly selected the principal curvatures of the membrane surface, the angle tangent to the surface of the membrane, and the rate of change of the membrane surface. It was found that the harder NPs were not easily deformed, and could thus be completely wrapped by the cell membrane. Conversely, softer NPs underwent deformation during internalization, and could consequently enter the cell, but not as easily as the harder NPs. In particular, the softer NPs underwent a shape deformation from spherical to ellipsoidal during internalization, which hinders the process; ellipsoidal NPs require 30% more energy compared to spherical-coated NPs. This further explains why harder non-deformable spherical NPs are easier to internalize into cells.

In another study, the coarse-grained molecular dynamics (CGMD) model was used to control energy changes in interactions between NPs and cell membranes by employing key parameters such as bonding, area, volume, and bending stiffness.[87] Soft NPs were found to be capable of adhering to, and diffusing into the cell membrane at an early stage due to the low bending energy (Fig. 4d and e). Therefore, in the early stage of film encapsulation, the softer NPs were found to internalize at a faster rate. Also, the elastic energy was found to modify significantly and the speed of

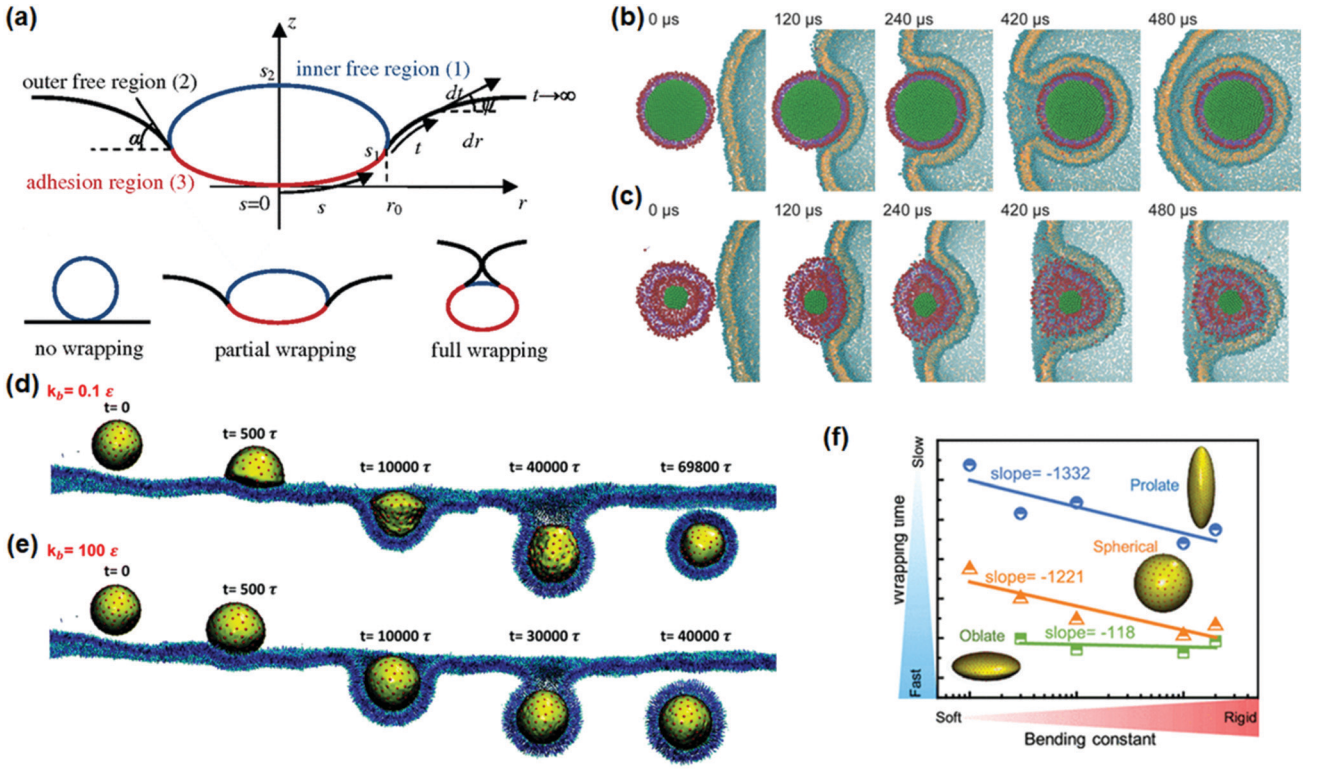

Fig. 4 Computational simulation analysis to investigate the internalization of elastic particles. (a) Schematic illustration of elastic particles wrapped by the cell membrane with relevant angles and arc lengths, and several particle wrapping states. MD simulations show the difference between hard (b) and soft (c) lipid particles that are internalized *via* the wrapping of the cell membrane as deformation influencing. The CGMD model shows the soft (d) and hard (e) elastic NPs during the membrane wrapping process. (f) Wrapping time as a function of bending constant for oblate, prolate, and spherical NPs. The arrangement of the encapsulation efficiency is oblate > spherical > prolate. (a) adapted from Yi *et al.* (2011). Copyright 2011 American Physical Society. (b) and (c) adapted from Sun *et al.* (2015). Copyright 2015 The Wiley-VCH. (d) and (e) adapted from Shen *et al.* (2018). Copyright 2018 Royal Society of Chemistry. (f) adapted from Shen *et al.* (2019). Copyright 2019 American Chemical Society.

film wrapping was found to be reduced. On the other hand, the study showed that the wrapping of harder NPs was much faster, compared to softer NPs. The simulated calculation phenomenon that the degree of internalization reverses with time is consistent with the experimental results earlier reported by Alexander *et al.*[63] The CGMD model was also used in a later study to assess the receptor-mediated membrane encapsulation process of elastic NPs with different sizes and shapes.[88] The authors found that the membrane encapsulation efficiency of elastic NPs is controlled by the receptor recruitment speed and free energy barrier, and the acceptor oligomerization rate is mainly determined by the receptor diffusion flux between the NPs and the membrane. The length of the contact edge and the free energy barrier were found to be dependent on the free energy of the NP and the membrane. This study also showed that softer spherical NPs are more difficult to internalize due to deformation, while under the same bending constant condition, the larger the size, the more difficult a particle's internalization becomes. More specifically, it was found that for the same bending constant, in the mode in which the tip is preferentially entered, the arrangement of the encapsulation efficiency is oblate NP > spherical NP > prolate NP (Fig. 4f). However, when the entry angle becomes a side-first entry mode, the order of package efficiency is reversed. The findings of this simulation may explain the contradictory results obtained in the frame of the experiment addressing the contact pattern of NPs with cells.

In a different work, Chen *et al.* developed a coarse-grained model using two-dimensional triangulation and observed that the elasticity and configuration deformation of NPs play important roles in regulating the kinetics of endocytosis by a tensionless membrane bilayer.[89] They found that the uptake kinetics of spherical and prolate NPs decreased by elasticity, however the uptake kinetics of oblate NPs increased. Further analysis revealed that the asymmetric morphology deformation decreases the mean curvature of the NP edge, due to the membrane suppression of the edge circumference. Furthermore, in the endocytic process of oblate NPs, the breaking of NP symmetry curvature decreases the active barrier and speeds up the reorientation step. However, this becomes an opposite effect in the endocytic process of prolate NPs.

Whether using the MD model or CGMD model, calculations can be very expensive and time consuming depending on the range of considerations when considering many cellular structural factors. Therefore, the current models available in the literature on the cellular uptake of NPs are still limited, and more complex computational simulation models need to be developed, benchmarked, and integrated. Moreover, cell structure factors can greatly improve the process of cellular uptake of NPs.

6. Summary and future perspectives

With the rapid development of nanotechnology, various classes of MNPs are becoming widely used in the biomedical field. The versatility in sizes, shapes, ligands, and types of such materials provides great opportunities for biological and clinical applications. However, their physical properties are also a cause of concern with regard to their influence on particle–cell interactions, taking cognizance of the key role of elasticity in drug delivery. Minutely studying the mechanism of MNP elasticity on cellular interaction necessitates further studies on their biological effect in order to design an appropriate scenario of the synthesis of functional MNPs toward a specific demand. Considerable progress has been recorded in understanding the interaction between different MNPs and cells, but there are some aspects that have not been addressed yet, which still need to be further unraveled.

Herein, we have summarized a series of results and conclusions of recent experiments that focused on understanding elasticity and its biological effect in the case of different types of MNPs, with various surface coatings, and sizes. An important finding of past performed work is that distinct elastic properties of MNPs with various physicochemical parameters can induce different pathways of cell phagocytosis, which include the clathrin-mediated phagocytosis, caveola-mediated phagocytosis, macropinocytosis, and cell membrane fusion, hence the uptake extent of MNPs depends on their elasticity modulus. In addition, upon phagocytosis, deformation of the MNPs occurs (especially in soft particles), and such shape modifications influence their uptake by cells. Micro and nano-sized systems behave very differently in terms of their biological interactions with cells, so we compared the results in one work, where all particles have similar physical and chemical properties, except the elasticity. Because each system uses different material types, sizes, and even shapes, it is difficult to compare the cellular uptake results between different systems directly. Furthermore, different computational simulation models introduced to assess the interaction between the deformation of MNPs and their cellular phagocytosis have been discussed for the comparison of different elasticities. The current models available in the literature on the cellular uptake of MNPs are still limited, and more complex computational simulation models need to be developed. First, it could be understood that the underlying mechanisms of elasticity's influence on the cellular uptake effect is multifold, and the correlation of many physicochemical parameters with elasticity cannot be straightforwardly understood. The MNP models used for the comparison did not have better defined properties that consist of full complexity of non-standard materials. A key limitation in better understanding the effects of MNPs' elasticity on their cellular uptake consists in the difficulty to change individual physicochemical properties of the compared MNPs while the others are kept constant. By precisely controlling the physicochemical parameters of MNPs, the impact of elasticity on the biological effect would be better investigated and more easily analyzed. However, for the estimation of elasticity of MNPs, the calculation range from Pa to GPa cannot be fully measured, owing to difficulties in their synthesis. An effective method, which can quantitatively measure the elastic modulus upon phagocytosis in real time, is required to elucidate the exact influence of this property on this process. In summary, this review offers an overview of past work that demonstrated the interrelationship that exists between MNPs' elasticity and their internalization in cells by different phagocytic pathways, highlighting the multitude of factors that are important to take into account in this context.

Conflicts of interest

There are no conflicts to declare.

Acknowledgements

The authors acknowledge the support of the National Key R&D Program of China (2018YFC0910601), the National Natural Science Foundation of China (51803228 and 31971292), the Zhejiang Provincial Natural Science Foundation of China (LGF18H180017) and the Ningbo Natural Science Foundation of China (2019A610192). Stefan G. Stanciu acknowledges the support of Romania's Executive Agency for Higher Education, Research, Development and Innovation Funding (UEFISCDI) *via* grants PN-III-P1-1.1-TE-2016-2147 (CORIMAG) and PN-III-P3-3.1-PM-RO-CN-2018-0177 (NANOMATBIOIMAGE).

References

1 S. Salatin, S. M. Dizaj and A. Y. Khosroushahi, *Cell Biol. Int.*, 2015, **39**, 881–890.
2 D. H. Jo, J. H. Kim, T. G. Lee and J. H. Kim, *Nanomedicine*, 2015, **11**, 1603–1611.
3 P. Foroozandeh and A. A. Aziz, *Nanoscale Res. Lett.*, 2018, **13**, 12.
4 A. C. Anselmo and S. Mitragotri, *Adv. Drug Delivery Rev.*, 2017, **108**, 51–67.
5 Y. Hui, X. Yi, F. Hou, D. Wibowo, F. Zhang, D. Y. Zhao, H. J. Gao and C. X. Zhao, *ACS Nano*, 2019, **13**, 7410–7424.
6 D. Septiadi, F. Crippa, T. L. Moore, B. Rothen-Rutishauser and A. Petri-Fink, *Adv. Mater.*, 2018, **30**, 30.
7 P. del Pino, F. Yang, B. Pelaz, Q. Zhang, K. Kantner, R. Hartmann, N. M. de Baroja, M. Gallego, M. Moller, B. B. Manshian, S. J. Soenen, R. Riedel, N. Hampp and W. J. Parak, *Angew. Chem., Int. Ed.*, 2016, **55**, 5483–5487.
8 Y. Hui, D. Wibowo, Y. Liu, R. Ran, H. F. Wang, A. Seth, A. P. J. Middelberg and C. X. Zhao, *ACS Nano*, 2018, **12**, 2846–2857.
9 N. G. Sosale, T. Rouhiparkouhi, A. M. Bradshaw, R. Dimova, R. Lipowsky and D. E. Discher, *Blood*, 2015, **125**, 542–552.
10 K. A. Beningo and Y. L. Wang, *J. Cell Sci.*, 2002, **115**, 849–856.
11 A. C. Anselmo, M. W. Zhang, S. Kumar, D. R. Vogus, S. Menegatti, M. E. Helgeson and S. Mitragotri, *ACS Nano*, 2015, **9**, 3169–3177.
12 L. Zhang, Q. Feng, J. L. Wang, S. Zhang, B. Q. Ding, Y. J. Wei, M. D. Dong, J. Y. Ryu, T. Y. Yoon, X. H. Shi, J. S. Sun and X. Y. Jiang, *ACS Nano*, 2015, **9**, 9912–9921.

13 H. L. Sun, E. H. H. Wong, Y. Yan, J. W. Cui, Q. Dai, J. L. Guo, G. G. Qiao and F. Caruso, *Chem. Sci.*, 2015, **6**, 3505–3514.
14 R. Hartmann, M. Weidenbach, M. Neubauer, A. Fery and W. J. Parak, *Angew. Chem., Int. Ed.*, 2015, **54**, 1365–1368.
15 X. Banquy, F. Suarez, A. Argaw, J. M. Rabanel, P. Grutter, J. F. Bouchard, P. Hildgen and S. Giasson, *Soft Matter*, 2009, **5**, 3984–3991.
16 J. W. Cui, R. De Rose, J. P. Best, A. P. R. Johnston, S. Alcantara, K. Liang, G. K. Such, S. J. Kent and F. Caruso, *Adv. Mater.*, 2013, **25**, 3468–3472.
17 M. R. Yu, L. Xu, F. L. Tian, Q. Su, N. Zheng, Y. W. Yang, J. L. Wang, A. H. Wang, C. L. Zhu, S. Y. Guo, X. X. Zhang, Y. Gan, X. F. Shi and H. J. Gao, *Nat. Commun.*, 2018, **9**, 11.
18 A. L. Becker, A. P. R. Johnston and F. Caruso, *Small*, 2010, **6**, 1836–1852.
19 J. P. Best, Y. Yan and F. Caruso, *Adv. Healthcare Mater.*, 2012, **1**, 35–47.
20 Z. J. Deng, S. W. Morton, E. Ben-Akiva, E. C. Dreaden, K. E. Shopsowitz and P. T. Hammond, *ACS Nano*, 2013, **7**, 9571–9584.
21 L. Sun, R. Riedel, S. G. Stanciu, F. Yang, N. Hampp, L. Xu and A. Wu, *J. Mater. Chem. B*, 2018, **6**, 2960–2971.
22 Y. Takechi-Haraya, Y. Goda, K. Izutsu and K. Sakai-Kato, *Anal. Chem.*, 2019, **91**, 10432–10440.
23 L. Y. T. Chou, K. Ming and W. C. W. Chan, *Chem. Soc. Rev.*, 2011, **40**, 233–245.
24 M. Mahmoudi, J. Meng, X. Xue, X. J. Liang, M. Rahman, C. Pfeiffer, R. Hartmann, P. R. Gil, B. Pelaz, W. J. Parak, P. del Pino, S. Carregal-Romero, A. G. Kanaras and S. T. Selvan, *Biotechnol. Adv.*, 2014, **32**, 679–692.
25 G. Sahay, D. Y. Alakhova and A. V. Kabanov, *J. Controlled Release*, 2010, **145**, 182–195.
26 G. J. Doherty and H. T. McMahon, *Annu. Rev. Biochem.*, 2009, **78**, 857–902.
27 H. Hillaireau and P. Couvreur, *Cell. Mol. Life Sci.*, 2009, **66**, 2873–2896.
28 B. M. F. Pearse, *Proc. Natl. Acad. Sci. U. S. A.*, 1976, **73**, 1255–1259.
29 T. F. Roth and K. R. Porter, *J. Cell Biol.*, 1964, **20**, 313–332.
30 J. P. Ferguson, S. D. Huber, N. M. Willy, E. Aygun, S. Goker, T. Atabey and C. Kural, *J. Cell Sci.*, 2017, **130**, 3631–3636.
31 S. D. Conner and S. L. Schmid, *Nature*, 2003, **422**, 37–44.
32 J. E. Hassinger, G. Oster, D. G. Drubin and P. Rangamani, *Proc. Natl. Acad. Sci. U. S. A.*, 2017, **114**, E1118–E1127.
33 T. Kirchhausen, *Annu. Rev. Biochem.*, 2000, **69**, 699–727.
34 M. Marsh and H. T. McMahon, *Science*, 1999, **285**, 215–220.
35 M. S. Robinson, *Trends Cell Biol.*, 2004, **14**, 167–174.
36 J. Z. Rappoport, *Biochem. J.*, 2008, **412**, 415–423.
37 T. Soldati and M. Schliwa, *Nat. Rev. Mol. Cell Biol.*, 2006, **7**, 897–908.
38 E. Cocucci, F. Aguet, S. Boulant and T. Kirchhausen, *Cell*, 2012, **150**, 495–507.
39 J. Dausend, A. Musyanovych, M. Dass, P. Walther, H. Schrezenmeier, K. Landfester and V. Mailander, *Macromol. Biosci.*, 2008, **8**, 1135–1143.
40 C. Brandenberger, C. Muhlfeld, Z. Ali, A. G. Lenz, O. Schmid, W. J. Parak, P. Gehr and B. Rothen-Rutishauser, *Small*, 2010, **6**, 1669–1678.
41 R. G. Parton and M. A. del Pozo, *Nat. Rev. Mol. Cell Biol.*, 2013, **14**, 98–112.
42 E. Boucrot, M. T. Howes, T. Kirchhausen and R. G. Parton, *J. Cell Sci.*, 2011, **124**, 1965–1972.
43 M. Stahlhut and B. van Deurs, *Mol. Biol. Cell*, 2000, **11**, 325–337.
44 S. A. Wickstrom, A. Lange, M. W. Hess, J. Polleux, J. P. Spatz, M. Kruger, K. Pfaller, A. Lambacher, W. Bloch, M. Mann, L. A. Huber and R. Fassler, *Dev. Cell*, 2010, **19**, 574–588.
45 T. Richter, M. Floetenmeyer, C. Ferguson, J. Galea, J. Goh, M. R. Lindsay, G. P. Morgan, B. J. Marsh and R. G. Parton, *Traffic*, 2008, **9**, 893–909.
46 R. G. Parton and K. Simons, *Nat. Rev. Mol. Cell Biol.*, 2007, **8**, 185–194.
47 H. Thorn, K. G. Stenkula, M. Karlsson, U. Ortegren, F. H. Nystrom, J. Gustavsson and P. Stralfors, *Mol. Biol. Cell*, 2003, **14**, 3967–3976.
48 Z. J. Wang, C. Tiruppathi, J. Cho, R. D. Minshall and A. B. Malik, *IUBMB Life*, 2011, **63**, 659–667.
49 J. Rejman, M. Conese and D. Hoekstra, *J. Liposome Res.*, 2006, **16**, 237–247.
50 A. Policard and M. Bessis, *Rev. Hematol.*, 1959, **14**, 487–495.
51 M. C. Kerr and R. D. Teasdale, *Traffic*, 2009, **10**, 364–371.
52 A. S. Desai, M. R. Hunter and A. N. Kapustin, *Philos. Trans. R. Soc., B*, 2019, **374**, 13.
53 N. Gunduz, H. Ceylan, M. O. Guler and A. B. Tekinay, *Sci. Rep.*, 2017, **7**, 10.
54 X. Q. Liu and D. Ghosh, *Int. J. Nanomed.*, 2019, **14**, 6589–6600.
55 J. Gilleron, W. Querbes, A. Zeigerer, A. Borodovsky, G. Marsico, U. Schubert, K. Manygoats, S. Seifert, C. Andree, M. Stoter, H. Epstein-Barash, L. G. Zhang, V. Koteliansky, K. Fitzgerald, E. Fava, M. Bickle, Y. Kalaidzidis, A. Akinc, M. Maier and M. Zerial, *Nat. Biotechnol.*, 2013, **31**, 638–646.
56 J. E. Rothman, *Angew. Chem., Int. Ed.*, 2014, **53**, 12676–12694.
57 J. Wilschut and D. Hoekstra, *Trends Biochem. Sci.*, 1984, **9**, 479–483.
58 N. Duzgunes and S. Nir, *Adv. Drug Delivery Rev.*, 1999, **40**, 3–18.
59 D. Luo and W. M. Saltzman, *Nat. Biotechnol.*, 2000, **18**, 33–37.
60 C. Francois-Martin, J. E. Rothman and F. Pincet, *Proc. Natl. Acad. Sci. U. S. A.*, 2017, **114**, 1238–1241.
61 S. Sabharanjak, P. Sharma, R. G. Parton and S. Mayor, *Dev. Cell*, 2002, **2**, 411–423.
62 J. G. Donaldson, N. Porat-Shliom and L. A. Cohen, *Cell. Signalling*, 2009, **21**, 1–6.
63 J. F. Alexander, V. Kozlovskaya, J. Chen, T. Kuncewicz, E. Kharlampieva and B. Godin, *Adv. Healthcare Mater.*, 2015, **4**, 2657–2666.
64 J. S. Sun, L. Zhang, J. L. Wang, Q. Feng, D. B. Liu, Q. F. Yin, D. Y. Xu, Y. J. Wei, B. Q. Ding, X. H. Shi and X. Y. Jiang, *Adv. Mater.*, 2015, **27**, 1402–1407.
65 J. W. Ma, Y. Zhang, K. Tang, H. F. Zhang, X. N. Yin, Y. Li, P. W. Xu, Y. L. Sun, R. H. Ma, T. T. Ji, J. W. Chen, S. Zhang, T. Z. Zhang, S. Q. Luo, Y. Jin, X. L. Luo, C. Y. Li, H. W. Gong, Z. X. Long, J. Z. Lu, Z. W. Hu, X. T. Cao, N. Wang, X. L. Yang and B. Huang, *Cell Res.*, 2016, **26**, 713–727.

66 S. E. Cross, Y. S. Jin, J. Rao and J. K. Gimzewski, *Nat. Nanotechnol.*, 2007, **2**, 780–783.
67 J. W. Myerson, B. Braender, O. McPherson, P. M. Glassman, R. Y. Kiseleva, V. V. Shuvaev, O. Marcos-Contreras, M. E. Grady, H. S. Lee, C. F. Greineder, R. V. Stan, R. J. Composto, D. M. Eckmann and V. R. Muzykantov, *Adv. Mater.*, 2018, **30**, 9.
68 W. J. Liu, X. Y. Zhou, Z. W. Mao, D. H. Yu, B. Wang and C. Y. Gao, *Soft Matter*, 2012, **8**, 9235–9245.
69 P. Guo, D. X. Liu, K. Subramanyam, B. R. Wang, J. Yang, J. Huang, D. T. Auguste and M. A. Moses, *Nat. Commun.*, 2018, **9**, 9.
70 C. Kinnear, T. L. Moore, L. Rodriguez-Lorenzo, B. Rothen-Rutishauser and A. Petri-Fink, *Chem. Rev.*, 2017, **117**, 11476–11521.
71 J. A. Champion and S. Mitragotri, *Proc. Natl. Acad. Sci. U. S. A.*, 2006, **103**, 4930–4934.
72 S. Dasgupta, T. Auth and G. Gompper, *Nano Lett.*, 2014, **14**, 687–693.
73 S. Y. Lin, W. H. Hsu, J. M. Lo, H. C. Tsai and G. H. Hsiue, *J. Controlled Release*, 2011, **154**, 84–92.
74 K. Supattarasakda, K. Petcharoen, T. Permpool, A. Sirivat and W. Lerdwijitjarud, *Powder Technol.*, 2013, **249**, 353–359.
75 D. Paul, S. Achouri, Y. Z. Yoon, J. Herre, C. E. Bryant and P. Cicuta, *Biophys. J.*, 2013, **105**, 1143–1150.
76 N. Doshi and S. Mitragotri, *PLoS One*, 2010, **5**, 6.
77 G. Sharma, D. T. Valenta, Y. Altman, S. Harvey, H. Xie, S. Mitragotri and J. W. Smith, *J. Controlled Release*, 2010, **147**, 408–412.
78 Y. Zhang, S. Tekobo, Y. Tu, Q. Zhou, X. Jin, S. A. Dergunov, E. Pinkhassik and B. Yan, *ACS Appl. Mater. Interfaces*, 2012, **4**, 4099–4105.
79 Z. Lu, Y. Qiao, X. T. Zheng, M. B. Chan-Park and C. M. Li, *MedChemComm*, 2010, **1**, 84–86.
80 L. Florez, C. Herrmann, J. M. Cramer, C. P. Hauser, K. Koynov, K. Landfester, D. Crespy and V. Mailander, *Small*, 2012, **8**, 2222–2230.
81 Z. G. Teng, C. Y. Wang, Y. X. Tang, W. Li, L. Bao, X. H. Zhang, X. D. Su, F. Zhang, J. J. Zhang, S. J. Wang, D. Y. Zhao and G. M. Lu, *J. Am. Chem. Soc.*, 2018, **140**, 1385–1393.
82 Y. Geng, P. Dalhaimer, S. S. Cai, R. Tsai, M. Tewari, T. Minko and D. E. Discher, *Nat. Nanotechnol.*, 2007, **2**, 249–255.
83 M. R. Yu, W. Y. Song, F. L. Tian, Z. Dai, Q. L. Zhu, E. Ahmad, S. Y. Guo, C. L. Zhu, H. J. Zhong, Y. C. Yuan, T. Zhang, X. Yi, X. H. Shi, Y. Gan and H. J. Gao, *Proc. Natl. Acad. Sci. U. S. A.*, 2019, **116**, 5362–5369.
84 Z. Dai, M. R. Yu, X. Yi, Z. M. Wu, F. L. Tian, Y. Q. Miao, W. Y. Song, S. F. He, E. Ahmad, S. Y. Guo, C. L. Zhu, X. X. Zhang, Y. M. Li, X. H. Shi, R. Wang and Y. Gan, *ACS Nano*, 2019, **13**, 7676–7689.
85 X. Yi, X. H. Shi and H. J. Gao, *Phys. Rev. Lett.*, 2011, **107**, 5.
86 M. Deserno, *Phys. Rev. E: Stat., Nonlinear, Soft Matter Phys.*, 2004, **69**, 14.
87 Z. Q. Shen, H. L. Ye and Y. Li, *Phys. Chem. Chem. Phys.*, 2018, **20**, 16372–16385.
88 Z. Q. Shen, H. L. Ye, X. Yi and Y. Li, *ACS Nano*, 2019, **13**, 215–228.
89 L. P. Chen, X. J. Li, Y. H. Zhang, T. W. Chen, S. Y. Xiao and H. J. Liang, *Nanoscale*, 2018, **10**, 11969–11979.
90 R. Palomba, A. L. Palange, I. F. Rizzuti, M. Ferreira, A. Cervadoro, M. G. Barbato, C. Canale and P. Decuzzi, *ACS Nano*, 2018, **12**, 1433–1444.

